

Comparison of Performance Multistage H-Type Darrieus Normal and Inverse Vertical Axis Wind Turbine with CFD Analysis

Muktar Sinaga¹, Amma Muliya Romadoni¹, Yoyon Ahmudiarto² and Arwanto²

¹Department of Mechanical Engineering, Universitas 17 Agustus 1945 Jakarta, Indonesia

²National Research and Innovation Agency (BRIN), Indonesia

Keywords: Performance, Multistage, H-type Darrieus, Vertical Axis Wind Turbine, Wind Energy, CFD.

Abstract: H-type Darrieus Vertical Axis Wind Turbine (VAWT) produce more power in high Tip Speed Ratio (TSR) than other VAWTs. However, the disadvantage is low generated power in TSR less than 1. The performance of H-type Darrieus Vertical Axis Wind Turbine was studied with Computational Fluid Dynamic (CFD) analysis. H-type normal design compared to the H-type inverse of darrieus Multistage Vertical Axis Wind Turbine. In CFD simulation, the Unsteady Reynolds Averaged Navier-Stokes (URANS) equations were used and the turbulence model was solved with SST k- ω model. It showed the results of the analytical analysis to be compared with normal and inverse H-type darrieus Multistage VAWT. The results are h-type normal darrieus VAWT produce more power in RPM 50 than h-type inverse darrieus VAWT. The h-type inverse darrieus VAWT produce more power in RPM 100 and 150 than h-type normal darrieus VAWT.

1 INTRODUCTION

According to their axis of rotation, wind turbines are often divided into two categories: Vertical Axis Wind Turbines (VAWT) and Horizontal Axis Wind Turbines (HAWT). Each variety offers benefits and drawbacks. HAWT outperforms VAWT in wind directions that are stable. On the other hand, VAWT performs better than HAWT under unstable wind situations. Rotor diameter, type of blade, and other factors also have an impact on performance.

The creation of HAWT, the VAWT type utilized as a substitute for HAWT, has been the subject of numerous studies since the 1970s. Given that the HAWT type is more efficient than the VAWT type, the market wishes to see a large-scale production of energy using this kind. Nonetheless, the VAWT type is more cost-effective than the HAWT type and is appropriate for usage in metropolitan areas where installation and maintenance must be made simple. VAWT has recently been applied for offshore as well as wind energy purposes. As an illustration, consider the Canadian Eole project, which uses the VAWT offshore application. Though Darrieus VAWT is theoretically less efficient than HAWT. On the other hand, the Darrieus VAWT has a number of advantages over a HAWT type on a big scale.

VAWT divided blades into two categories: Savonius and Darrieus. Drag types are Savonius type and lift types are Darrieus type. Innovation is still needed, though, to enhance the performance of VAWT in areas like angle of attack, blade design, and other areas. Thus, in order to make improvements, the parameters need to be examined. Computational fluid dynamic (CFD) simulation is one of the numerical techniques used to innovate in VAWT. It will be simpler to innovate on the VAWT design by utilizing CFD simulation. Its cost can be decreased to facilitate analysis. When VAWT is applied in the field, the simulation's results can be utilized to forecast actual conditions.

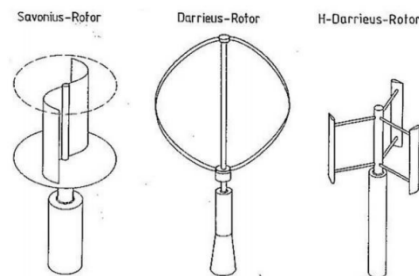


Figure 1: VAWT type in wind turbine.

The study of Computational Fluid Dynamics (CFD) uses digital computers to generate quantitative

predictions of fluid-flow phenomena based on the conservation laws (mass, momentum, and energy conservation) that govern fluid motion. Although CFD is becoming more and more important, its predictions are never totally accurate. When analyzing the findings of CFD techniques, caution must be exercised because there are numerous possible sources of mistake that could be implicated. Converting the partial differential equations governing a physical phenomenon into an algebraic system of equations is the cornerstone to many numerical techniques. There are various methods available for this conversion.

CFD is only a tool for fluid-flow problem analysis. When utilized appropriately, it may rapidly and affordably offer important information. The fundamentals of the finite-difference and finite-element approaches, as well as their uses in CFD. Other numerical techniques that are frequently employed in CFD include the spectrum approach and the spectral element method. They are similar in that they discretize the Navier-Stokes equations into an algebraic system of equations.

Energy equations, Navier-Stokes equations, and continuity equations are the common governing equations in computational fluid dynamics (CFD). This study examines three-dimensional, unstable, incompressible, and viscous flow phenomena with objects. The findings are in the form of moving frames because the model was simulated in the moving (rotation) domain. Consequently, the model's Reynold-Averaged Navier-Stokes equation.

The basic mass conservation equation is known as the continuity equation. A change in mass in the volume control (CV) equal to the net rate of mass entering CV is known as the law of mass conservation. The following is the mass conservation equation in integrals:

$$\frac{\partial}{\partial t} \int_{CV} \rho \cdot dV + \int_{CS} \rho \mathbf{u} \cdot \mathbf{n} \cdot dA = 0, \forall \mathbf{v} \in R$$

ρ is density (Kg/m³), u is flow velocity (m/s), and ∇ is divergence term.

The Navier-Stokes equation in incompressible viscous flow is described by the following equation:

$$\begin{aligned} \frac{\partial \bar{u}_i}{\partial t} + \bar{u}_j \frac{\partial \bar{u}_i}{\partial x_j} &= - \frac{\partial \bar{p}}{\partial x_i} + \nu \frac{\partial^2 \bar{u}_i}{\partial x_j \partial x_j} - \frac{\partial \tau_{ij}}{\partial x_j} \\ \tau_{ij} &= \bar{u}_i \bar{u}_j \\ \frac{\partial \bar{u}_i}{\partial x_i} &= 0 \end{aligned}$$

Where u_i is fluid velocity (m/s), p is pressure (Pa), and ν is kinematic viscosity (m²/s).

2 METHODS

First, the geometry is described in this section. The blade design model that will be examined using CFD software. Three primary steps comprise CFD analysis are pre-processing, processing, and post-processing. Following the creation of the blade design, the computational and rotating domains were created. After that, the ANSYS program is prepared to simulate the design.

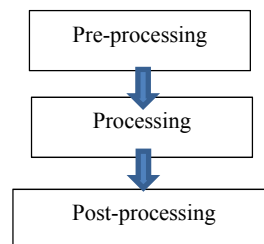


Figure 2: Step of CFD analysis.

A. Pre-processing

In the pre-processing stage, the design of multistage VAWT was built and then simulate in ANSYS CFD software. H-type VAWT Blade design taken from NACA 4212 prototype. The design is appropriate for VAWT and has a good drag.

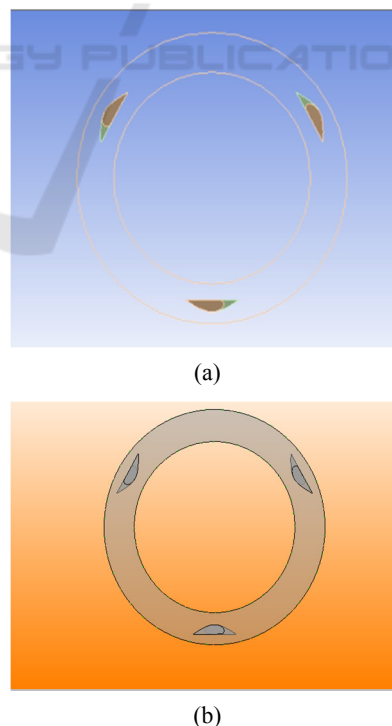


Figure 3: H-type VAWT (a) Normal and (b) inverse blade.

The design of blade VAWT is h-type Darrieus with normal and inverse position. The design of VAWT blade has a rotor diameter of 2.5 m and the total height of multistage vawt is 9.5 m. The angle of attack 0°, 40°, and 80° and with 3 number of blades.

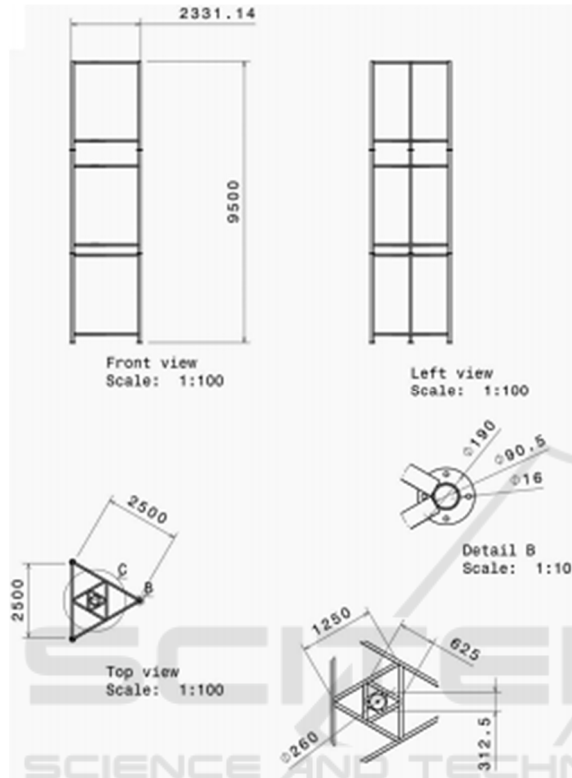


Figure 4: Design of multistage VAWT.

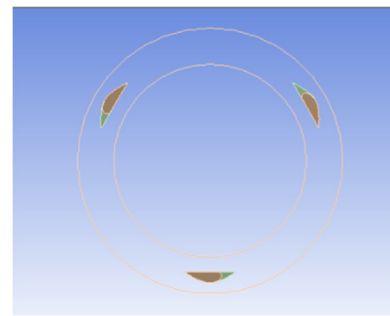
B. Processing

The ANSYS package with Fluent's CFD software is used in this study's numerical setting. VAWT's unique blade is simulated using ANSYS. The incompressible unstable model Reynolds-averaged Navier-Stokes (RANS) equations are utilized since the objects are simulated as being unsteady. Shear Stress Transport (SST) hybrid $k-\omega$ is the chosen turbulent model. The wind speed represented in the simulation's velocity inlet 7 m/s. The RPM are 50, 100, and 150. Operating pressure at one atmosphere, or ordinary atmospheric pressure. Air has a density of 1.1839 Kg/m^3 .

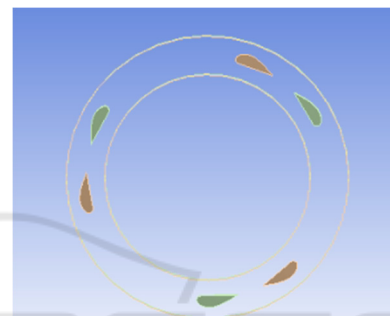
C. Post-processing

The next step is to examine the results that obtained from the simulation stage. The data from simulation of CFD including streamlines, vector plots, and

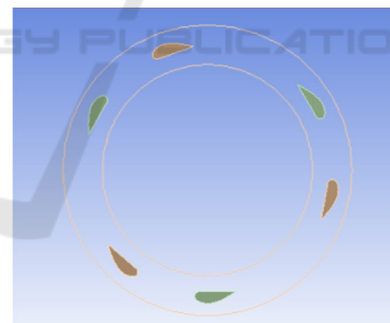
contour plots. From the data, performance (power) of VAWT can be calculated from the value of torque in the simulation ($P = T * \omega$).



(a)



(b)



(c)

Figure 5: Contra rotating multistage VAWT blade. (a) 0, (b) 40 and (c) 80 degrees.

3 RESULTS AND DISCUSSION

The performance of h-type multistage VAWT was determined from the results of the CFD simulation. The torque measured during 360-degree rotations at various RPM. The power displayed in table 1 and Fig. 8 for various RPM. Velocity and pressure contour displayed in Fig. 6 and 7.

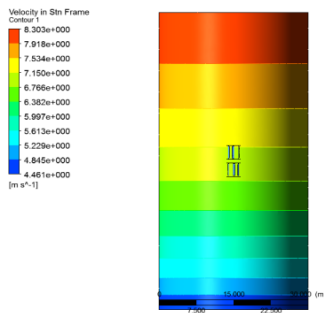


Figure 6: Velocity contour at boundary condition.

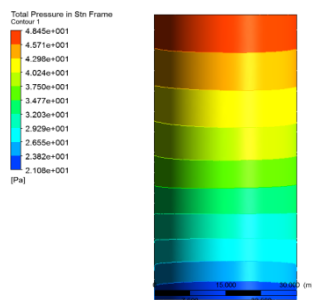


Figure 7: Pressure contour at boundary condition.

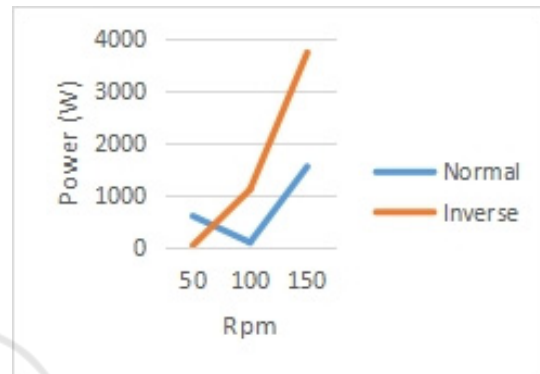
Table 1: Results of CFD analysis.

DEGREE	RPM	NORMAL (W)	INVERSE (W)
0	50	591.06	24.55684
	100	83.06	1102.471216
	150	1544.0964	3737.24736
40	50	391.804644	185.5287588
	100	154.30492	922.803112
	150	1680.756	3765.05052
80	50	348.042156	37.217488
	100	340.4520504	1468.635168
	150	1680.756	5558.58996

At 0-degree, h-type normal VAWT has better power output (591.06 W) than h-type inverse VAWT (24.56 W) at 50 RPM. But, at 100 and 150 RPM h-type inverse VAWT has better power output than h-type normal VAWT. In 100 RPM, h-type normal VAWT has power output 83.06 W and h-type inverse VAWT has power output 1102.47 W. In 150 RPM, h-type normal VAWT has power output 1544.10 W and h-type inverse VAWT has power output 3737.25 W.

At 40-degree, h-type normal VAWT has better power output (391.80 W) than h-type inverse VAWT (185.53 W) at 50 RPM. But, at 100 and 150 RPM h-type inverse VAWT has better power output than h-type normal VAWT. In 100 RPM, h-type normal VAWT has power output 154.30 W and h-type inverse VAWT has power output 922.80 W. In 150 RPM, h-type normal VAWT has power output 1680.76 W and h-type inverse VAWT has power output 3765.055 W.

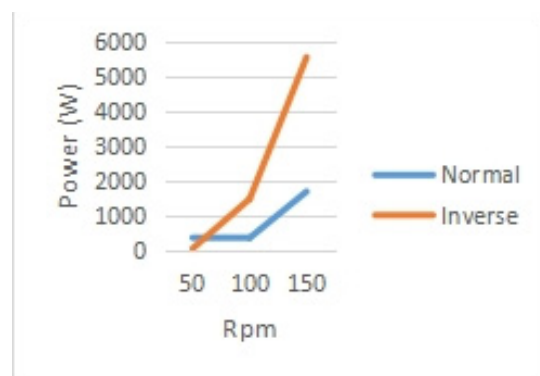
At 80-degree, h-type normal VAWT has better power output (348.04 W) than h-type inverse VAWT (37.22 W) at 50 RPM. But, at 100 and 150 RPM h-type inverse VAWT has better power output than h-type normal VAWT. In 100 RPM, h-type normal VAWT has power output 340.45 W and h-type inverse VAWT has power output 1468.63 W. In 150 RPM, h-type normal VAWT has power output 1680.76 W and h-type inverse VAWT has power output 5558.59 W.



(a)



(b)



(c)

Figure 8: Graphic of RPM vs Power at (a) 0 °, (b) 40 °, and (c) 80 °.

4 CONCLUSION

In this study, h-type multistage VAWT analyzed with a numerical method using Computational Fluid Dynamic (CFD) analysis. The conclusion of the analysis is h-type normal darrieus VAWT produce more power in RPM 50 than h-type inverse darrieus VAWT. Then, h-type inverse darrieus VAWT produce more power in RPM 100 and 150 than h-type normal darrieus VAWT. Therefore, h-type normal darrieus suitable for low RPM (50 Rpm) in multistage VAWT. In the future research refers to compare with several type of VAWT design.

REFERENCES

- Admono, T., et. al. (2020). Numerical investigation of the effect of triangle strut in vertical axis wind turbine (VAWT). *Journal of Mechatronics, Electrical Power, and Vehicular Technology*.
- Ahmudiarto, Y., et. al. (2019). Performance Analysis of Novel Blade Design of Vertical Axis Wind Turbine. *International Conference on Sustainable Energy Engineering and Application (ICSEEA)*.
- Ahmudiarto, Y., et. al. Performance and Productivity Enhancements on Vertical Axis Wind Turbine with a Novel multi-stages Contra-rotating Technique. *International Conference on Sustainable Energy Engineering and Application (ICSEEA)*.
- Al-Ghriybah1, M., Didane, D. H. (2023). Performance Improvement of a Savonius Wind Turbine using Wavy Concave Blades. *Semarak Ilmu Publishing, Malaysia, Issue 9*.
- Baharudin, M. A. A., et. al. (2020). CFD Simulation Study of Multistage Vertical Axis Wind Turbine (VAWT). *Advances in Mechanical, Manufacturing and Aerospace Engineering, Malaysia, Series 1*.
- D. H. Didane, et. al. (2019). Performance Investigation of a Small Savonius Darrieus counter Rotating vertical Axis Wind Turbine. *International Journal energy Res.*
- Hau, E. (2006). *Wind Turbines: Fundamentals, Technologies, Application, Economics*. Springer. 2nd ed.
- M. Zcmamou, M. Aggour, A. Toumi. (2017) Review of Savonius Wind Turbine Design and Performance. *International Conference on Power and Energy Systems Engineering*
- N.C. Batista, R. Melicio, J.C.O. Matias, J.P.S. Catalão. (2011). Self-Start Evaluation in Lift-Type Vertical Axis Wind Turbines: Methodology and Computational Tool Applied to Asymmetrical Airfoils. *International Conference on Power Engineering, Energy and Electrical Drives*.
- Tey Wah-Yen, Yutaka Asako, Nor Azwadi Che Sidik, Goh Rui-Zher. (2017) Governing Equations in Computational Fluid Dynamics: Derivations and A Recent Review. *Journal of Progress in Energy and Environment*. vol. 1, pages 1 – 19.